

## ARTICLE

## SYSTEM BIOLOGY AND IMMUNOGENETICS

# Bone marrow microenvironment drives AML cell OXPPOS addiction and AMPK inhibition to resist chemotherapy

Ruolan You<sup>1</sup> | Diyu Hou<sup>1</sup> | Bin Wang<sup>1</sup> | Jingru Liu<sup>1</sup> | Xiaoting Wang<sup>1</sup> |  
Qirong Xiao<sup>2</sup> | Zhipeng Pan<sup>1</sup> | Dongliang Li<sup>3</sup> | Xiaoming Feng<sup>4</sup> | Lixia Kang<sup>1</sup> |  
Ping Chen<sup>2</sup> | Huifang Huang<sup>1</sup>

<sup>1</sup> Central Laboratory, Fujian Medical University Union Hospital, Fuzhou, Fujian, China

<sup>2</sup> Fujian Institute of Hematology, Fujian Provincial Key Laboratory of Hematology, Fujian Medical University Union Hospital, Fuzhou, Fujian, China

<sup>3</sup> Department of Hepatobiliary Disease, The 900th Hospital of the People's Liberation Army Joint Service Support Force, Fuzhou, Fujian, China

<sup>4</sup> State Key Laboratory of Experimental Hematology, Institute of Hematology and Hospital of Blood Diseases, Chinese Academy of Medical Sciences & Peking Union Medical College, Tianjin, China

## Correspondence

Huifang Huang, Central Laboratory, Fujian Medical University Union Hospital, 29 Xinquan Road, Fuzhou, Fujian 350001, China.  
Email: [huanghuif@fjmu.edu.cn](mailto:huanghuif@fjmu.edu.cn)

## Abstract

The stromal niche plays a pivotal role in AML chemoresistance and energy metabolism reprogramming is a hallmark of a tumor. 5'-Adenosine monophosphate-activated protein kinase (AMPK) is an important energy sensor suppressing mammalian target of rapamycin complex 1 (mTORC1) activity. However, the role of AMPK-mTORC1 pathway on connecting AML cell energy metabolism reprogramming and chemoresistance induced by the bone marrow microenvironment (BMM) is not defined. Here, with a co-culture system that simulates the interaction between BMM and AML cells, it is shown that stromal contact led to a decreased sensitivity to chemotherapy accompanied by an increase of oxidative phosphorylation (OXPHOS) activity and mitochondrial ATP synthesis in AML cells. The increased OXPPOS activity and excessive ATP production promoted chemoresistance of AML cells through inhibiting AMPK activity and in turn activating mTORC1 activity. In an in vivo AML mouse model, depletion of AMPK activity with genetic targeting promoted AML progression and reduced their sensitivity to chemotherapeutic drugs. Collectively, AML cells' acquired increased OXPPOS activity as well as AMPK inhibition could be therapeutically exploited in an effort to overcome BMM-mediated chemoresistance.

## KEYWORDS

acute myeloid leukemia, AMPK-mTORC1 pathway, ATP, chemotherapy resistance, OXPPOS

## 1 | INTRODUCTION

Acute myeloid leukemia (AML) is a malignant disorder characterized by clonal expansion of abnormally differentiated myeloid lineage cells.<sup>1,2</sup> The long-term survival of AML patients is still poor as most patients

ultimately relapse despite achieving remission.<sup>3,4</sup> The existence of chemotherapy-resistant AML clones in the bone marrow (BM) is a major source of disease recurrence.<sup>5,6</sup> Stromal cells in the bone marrow microenvironment (BMM) have been reported to play key roles in promoting chemoresistance of the leukemia cells.<sup>7-10</sup> However, how bone marrow stromal cells (BMSCs) induced AML chemoresistance remains unclear.

Energy metabolism reprogramming is an emerging hallmark of tumor cells.<sup>11,12</sup> The discovery of the Warburg effect has drawn

**Abbreviations:** 4E-BP1, eukaryotic initiation factor 4E-binding proteins 1; AICAR, 5-aminoimidazole-4-carboxamide ribonucleotide; AML, acute myeloid leukemia; AMPK, 5'-adenosine monophosphate-activated protein kinase; Ara-C, cytarabine; BMM, bone marrow microenvironment; DNR, daunorubicin; mTORC1, mammalian target of rapamycin complex 1; NC, negative control; OE, overexpression; OXPPOS, oxidative phosphorylation; p70S6K, ribosomal protein kinase S6; WT, wild-type

This is an open access article under the terms of the [Creative Commons Attribution-NonCommercial-NoDerivs](https://creativecommons.org/licenses/by-nc-nd/4.0/) License, which permits use and distribution in any medium, provided the original work is properly cited, the use is non-commercial and no modifications or adaptations are made.

© 2021 The Authors. *Journal of Leukocyte Biology* published by Wiley Periodicals LLC on behalf of Society for Leukocyte Biology.

increasing attention to the role of aerobic glycolysis in cancer cells.<sup>13</sup> However, in recent years, the analysis of particularly aggressive and drug-resistant cancers has demonstrated that the survival of tumor cells strongly depended on oxidative phosphorylation (OXPHOS), rather than glycolysis.<sup>14</sup> Previous studies have suggested that chemo-resistant AML cells exhibited high OXPHOS activities,<sup>15</sup> and relied on OXPHOS for survival, and that blocking OXPHOS increased AML cells chemosensitivity.<sup>16</sup>

The main function of mitochondrial OXPHOS is to produce ATP to provide energy in a cell. AMPK is allosterically activated by phosphorylation at a threonine site 172 (T172) within  $\alpha$  subunit to respond to increased AMP/ATP ratio<sup>17,18</sup> and negatively controls the protein synthesis and cell growth by restraining the activity of Mammalian target of rapamycin complex 1 (mTORC1).<sup>19</sup> mTORC1 promotes protein synthesis, cell growth, and survival by phosphorylating eukaryotic initiation factor 4E-binding proteins (4E-BPs) and ribosomal protein kinase S6 (p70S6K). Upon phosphorylation by mTORC1, 4E-BP1 releases eukaryotic translation initiation factor 4E (eIF4E) and enhances 5' cap-dependent translation of mRNAs. This results in the increased translation of pro-survival proteins such as c-Myc, which ultimately promotes the survival of tumor cells.<sup>19-22</sup> The activation of AMPK was reported to promote tumor cells apoptosis by inhibiting mTORC1,<sup>23,24</sup> while mTORC1 pathways have been reported to be involved in the development of AML.<sup>25</sup> But it is unknown how the AMPK-mTORC1 pathway in AML is regulated by intrinsic and extrinsic signals. We sought to identify AMPK-mTORC1 pathways connecting BMM, AML cell energy metabolism reprogramming, and chemoresistance.

In this study, we sought to identify novel molecular pathways connecting AML cell energy metabolism reprogramming to chemoresistance induced by BMM. We found that stromal contact rendered AML cells higher OXPHOS activity and more mitochondrial ATP synthesis, which triggered the reduction of AMPK activity and increase of mTORC1 activity, resulting in the insensitivity of AML cells to chemotherapy. Our study reveals a novel mechanism of AML chemoresistance from the perspective of energy metabolism, which might have implications in AML treatment.

## 2 | MATERIALS AND METHODS

### 2.1 | Patient samples

This study was approved by the Committee for the Ethical Review of Research, Fujian Medical University Union Hospital (2018KY061) and informed consent was obtained from all the bone marrow providers. Human BM aspirates were collected from AML patients prior to treatment at Fujian Medical University Union Hospital, Fuzhou, China. Details on AML patient samples are shown in Table 1. AML blasts were purified using CD34 microbeads (Miltenyi Biotec, Shanghai, China). CD34<sup>+</sup> hematopoietic stem cells (HSCs) were obtained from BM of healthy donors and were purified using CD34 microbeads.

**TABLE 1** Patients' Information

No.	Gender/Age (year)	FAB type	AML cells in bone marrow (%)	WBC (10 <sup>9</sup> /L)	Hb (g/L)	PLT (10 <sup>9</sup> /L)	Cytogenetic profile	Mutation status
AML#1	Male/51	M5	72.1	80.08	56.0	5	46,XY[20]	None
AML#2	Male/46	M5	69.5	15.22	57.0	10	46,XY[20]	None
AML#3	Female/48	M5	95.3	71.38	51.0	18	46,XX[20]	CEBPA
AML#4	Male/53	M4Eo	66.7	199.4	61.0	16	46,XY,inv(16)(p13q22)[20];CBF $\beta$ -MYH11	NRAS; TET2; ASXL1; TP53; WT1
AML#5	Male/29	M5	59.6	283.96	65.0	13	46,XY;CBF $\beta$ -MYH11	WT1
AML#6	Male/17	M5	47.8	139.89	50.0	54	46,XY[20]	None
AML#7	Female/72	M2	87.5	48.21	51.0	37	46,XX[20]	TP53
AML#8	Female/50	M5	95.1	6.71	117.0	55	46,XX[20];FLT3-ITD	CEBPA; GATA2; IDH2; WT1; TET2
AML#9	Female/48	M5	89.7	206.81	56.0	37	46,XX[20];MLL-PTD	None
AML#10	Male/55	M5	27.2	183.58	47.0	42	46,XY[20];FLT3-ITD	None

WBC, white blood cell; HB, hemoglobin; PLT, platelet.

## 2.2 | Cell lines and culture condition

Cells were cultured at 37°C in a humidified atmosphere containing 5% CO<sub>2</sub>. Human AML cell lines (U937 and HL-60), purchased from the Cell Bank of Type Culture Collection of the Chinese Academy of Sciences (Shanghai, China), were maintained in medium RPMI-1640 (HyClone, Logan, UT) supplemented with 10% FBS (Gemini Bio-Products, Sacramento, CA, USA). HS-5 cells, a line of BMSCs, were purchased from the American Type Culture Collection (ATCC, Manassas, VA) and cultured in medium Dulbecco's Modified Eagle's Medium (DMEM/High, HyClone, Logan, UT) supplemented with 10% FBS. For primary AML cells, they were isolated and cultured in medium RPMI-1640 with 20% FBS.

## 2.3 | Establishment of co-culture system

To simulate the interaction between BMM and AML cells, direct contact co-culture system and non-contact co-culture system were established *in vitro*. For the direct contact co-culture system, HS-5 cells were seeded at  $1.0 \times 10^5$  per well in a 6-well plate and were left to adhere and proliferate until 70% confluency. Then, the supernatant was discarded, and AML cells were placed on the HS-5 cells at  $3.5 \times 10^5$  per well in medium RPMI-1640 supplemented with 10% FBS. The AML cells expressing human CD45 were selected by magnetic-activated cell sorting (MACS) (Miltenyi Biotec, Shanghai, China) after 24 h. For the non-contact co-culture system using transwell, AML cells were added into transwell with an aperture of  $1 \mu\text{M}$  to establish a noncontact co-culture system with HS-5 cells.

## 2.4 | Pharmacological agents

Cytarabine (Ara-C, Pharmacia, Italy) and daunorubicin (DNR, New Era Pharmaceutical Co. LTD, Shandong, China) were obtained from the central pharmacy of Fujian Medical University Union Hospital, Fuzhou, China. Oligomycin A, 5-aminoimidazole-4-carboxamide ribonucleotide (AICAR), and Compound C were purchased from MedChemExpress (Monmouth Junction, NJ, USA).

## 2.5 | Mitochondrial respiration and ATP measurement

To evaluate the OXPHOS activities and ATP synthesis, the oxygen consumption rate (OCR) was measured by using a Seahorse XFe24 bioanalyzer (Agilent Technologies, Santa Clara, California, USA). The basal respiration, maximal respiration, and spare respiratory capacity were examined as OXPHOS indexes. The basal respiration reflects the energetic demand of cells under basal conditions. Maximal respiration indicates the maximum rate of respiration that cells can achieve. The real-time ATP rate assay is designed to measure total ATP production rates in living cells. Even more relevant is the ability of this assay to distin-

guish the fractions of ATP from mitochondrial OXPHOS or glycolysis, the two main metabolic pathways responsible for ATP production in mammalian cells. Briefly, AML cells were cultured with or without HS-5 cells and then removed from the co-cultures and plated in cell-Tak coated XFe24 Cell Culture Microplates (Agilent Technologies) at a density of  $2 \times 10^5$  per well in basal medium containing 2.0 mM glucose, 1.0 mM Glutamine, 2.0 mM pyruvate, and 2.0 mM HEPES. The Seahorse XF Mito Stress test kit (Agilent Technologies) and Seahorse XF real-time ATP rate assay kit (Agilent Technologies) were employed to evaluate the levels of mitochondrial respiration and ATP synthesis. To analyze mitochondrial respiration, Oligomycin A ( $1 \mu\text{M}$ ), fluorocarbonyl cyanide phenylhydrazone (FCCP,  $2 \mu\text{M}$ ), and Rotenone/Antimycin A ( $0.5 \mu\text{M}$ ) were added to the injection ports. To evaluate ATP synthesis, oligomycin A ( $1.5 \mu\text{M}$ ) and rotenone/antimycin A ( $0.5 \mu\text{M}$ ) were used.

## 2.6 | Cell viability assay

Cell viability assays were performed to assess the sensitivity of AML cells to Ara-C and DNR. The cell viability was assessed with Cell Counting Kit-8 (CCK-8; Do Jindo Laboratories, Kumamoto, Japan) according to the manufacturer's instructions. After measuring optical density (OD) at 450/630 nm, the growth inhibition rate was calculated as follows: Inhibition rate (%) = (mean OD<sub>450-630</sub> of negative control cells - mean OD<sub>450-630</sub> of drug-treated cells) / (mean OD<sub>450-630</sub> of negative control cells - mean OD<sub>450-630</sub> of blank control cells)  $\times$  100%.

## 2.7 | Real-time fluorescence quantitative PCR

Total RNA was extracted from cells with TRIzol reagent (Invitrogen; Thermo Fisher Scientific) by following the manufacturer's protocol. The level of AMPK mRNA was quantified by RT-qPCR using an SYBR Premix Ex Taq (Roche Applied Science, Basel, Switzerland) and normalized to  $\beta$ -Actin expression. The sequence of AMPK-specific primers was as follow: forward 5'-GCTTTTCAGGCATCCTCAT-3', and reverse 5'-CATCCAGCCTTCCATTCTT-3'. The primers for  $\beta$ -Actin were: forward 5'-CCAACCGCGAGAAGATGA-3', and reverse 5'-TCCATCACGATGCCAGTG-3'.

## 2.8 | Western blot analysis

Cells were harvested and lysed in RIPA buffer (Dingguochangsheng, Beijing, China), containing PMSF (CST, Cell Signaling Technology, Danvers, MA, USA), protease inhibitor cocktail, and phosphatase inhibitor cocktail (CST). Equal amounts of protein extracts were resolved on 12% SDS polyacrylamide gel electrophoresis and transferred to 0.45- $\mu\text{M}$  PVDF membranes. The membranes were blocked with 10% nonfat dry milk in 1 $\times$ Tris-buffered saline containing 0.4% Tween-20. Membranes were probed with Ag-specific Abs. Anti-AMPK, anti-phospho-AMPK<sup>T172</sup>, anti-p70S6K, anti-phospho-p70S6K<sup>T389</sup>, anti-4E-BP1, anti-phospho-4E-BP1<sup>S65</sup>, and anti-c-Myc Abs were purchased

from CST; anti- $\beta$ -Actin were from Beyotime Biotechnology, Chain. The membrane-bound primary Abs were detected with HRP-conjugated goat anti-mouse or goat anti-rabbit secondary Abs (Beyotime Biotechnology). HRP activity was detected with a chemiluminescence detection kit (BOSTER, China). Images were obtained by using ImageLab Software (Bio-Rad, Hercules, CA, USA).

## 2.9 | Lentivirus production and infection

MSCV vector coexpressing human AMPK and zsGreen (pHBLV-CMV-MCS-3FLAG-EF1-ZsGreen-T2A-PURO) was purchased from Hanheng, Shanghai, China. The AMPK-targeting single guide (sg) RNA sequences (AMPK exon 1, sg1: 5'-GAAGATCGGCCACTACATTC-3'; sg2: 5'-TACATTCTGGGTGACACGCT-3') were synthesized by Sangon Biotech (Shanghai, China). LentiCRISPRv2 was a gift from Brett Stringer (RRID: Addgene\_98290). Lentiviral vectors expressing AMPK-targeting sgRNAs were generated as reported,<sup>26</sup> and verified by DNA sequencing. HEK-293T cells were transfected with pMD2.G, psPAX2, and target plasmids using lipofector3000 (Promega, Madison, WI, USA). The lentiviral supernatant was harvested at 48 h posttransfection and HEK-293T cells were replenished with fresh media for another harvest at 72 h posttransfection. The empty vectors were used as a negative control (NC). The AML cell lines were infected by the produced lentiviral particles. AML cells knocked out AMPK (AMPK-sg1/2) or stable overexpressing AMPK (AMPK-OE) were selected in the presence of puromycin (2.5  $\mu$ g/mL; Sigma-Aldrich, St. Louis, MO, USA) for 10 days. The efficiency of AMPK knockout was verified by western blot, while the efficiency of AMPK overexpression was assessed by both RT-qPCR and western blot.

## 2.10 | Flow cytometry

All flow cytometry (FCM) studies were performed using single-cell suspensions, and cells were stained in accordance with the standard protocols. The cytotoxic response was determined by measuring apoptosis after staining with AnnexinV-allophycocyanine (APC) and AAD (KeyGEN BioTECH, Jiangsu, China). The percentage of human CD45<sup>+</sup> cells in tissues was determined by using APC fluorescent dye-conjugated human CD45 Ab (BD-Biosciences, NJ, USA).

## 2.11 | AML xenografts in NCG mice

All experiments involving animals were performed according to protocols approved by the Committee of Research Animals of Fuzhou General Hospital of Nanjing Military Command (2020-044). NOD/SCID/IL-2ry<sup>null</sup> (NCG) mice were purchased from Model Animal Research Center of Nanjing University to evaluate the role of AMPK in disease progression and chemosensitivity. Human AML cells were injected in each mouse by tail vein in a final volume of 200  $\mu$ L PBS. The livers, spleens, and femurs were analyzed with human CD45 Ab conjugated with APC

fluorescent dye. For in vivo treatment of xenografts, day 3 of the transplant, the mice received Ara-C (5 mg/kg intravenously) once every 2 days, 3 times in all. The relative number of human CD45<sup>+</sup> cells was expressed as the ratio of the human CD45<sup>+</sup> cell proportion in the treated group to that in the untreated group.

## 2.12 | Immunofluorescence labeling and imaging

Fresh mouse tissues were fixed in 4% paraformaldehyde and embedded in paraffin. The tissue sections (4  $\mu$ M) were stained with hematoxylin and eosin (H&E) and analyzed by light microscopy (DM2500, Leica, Germany). For IF staining, the tissue sections were incubated with sodium citrate buffer for Ag retrieval, and then for 30 min in blocking solution containing 1 $\times$  PBS and 2% BSA (GenView, Shanghai, China), followed by overnight incubation with anti-human CD45 (1:50; Abcam, Cambridge, UK) at 4°C; then, the slides were incubated for 1 h at 25°C with a goat-raised secondary Ab conjugated to Alexa Fluor-488 (1:200 in blocking buffer) (Abcam, Cambridge, UK). The slides were washed 3 times in 0.5% PBST (1 $\times$ PBS, 0.5% Tween-20) before staining for 1 min with the nuclear marker, DAPI (Abcam, Cambridge, UK). Then, the slides were washed 4 times in 0.5% PBST, covered with a glass coverslip, left to dry in the dark, and their edges sealed with nail hardener. Images were obtained using a Leica and analyzed using Image J.

## 2.13 | Statistical analysis

All data were presented as means  $\pm$  standard deviation ( $-x \pm SD$ ) from 3 independent experiments. Statistical analyses were performed by applying variance and Student's t-test using SPSS statistical software version 19. *P*-values below 0.05 were considered indicative of statistical significance (\**P* < 0.05, \*\**P* < 0.01, \*\*\**P* < 0.001). For the analysis of western blot data, representative images of 3 independent experiments were used.

# 3 | RESULTS

## 3.1 | Coculture of AML cells with HS-5 cells exhibited higher OXPHOS activity and increased ATP synthesis

Primary CD34<sup>+</sup> blasts from AML patients exhibited significantly increased maximal respiration and spare respiratory capacity compared to CD34<sup>+</sup> cells from healthy donors (Fig. 1A and B). We hypothesized that the high OXPHOS activity was a characteristic of AML cells in BMM. To investigate the impact of BMM on OXPHOS in AML cells, we established two co-culture modes, one was direct contact co-culture system and the other was non-contact co-culture system through transwell, to simulate the interaction between AML cells and BMM. Two distinct leukemia cell lines, U937 and HL-60, were contact co-cultured with HS-5 cells, which were a BM-derived stromal cells line (result-

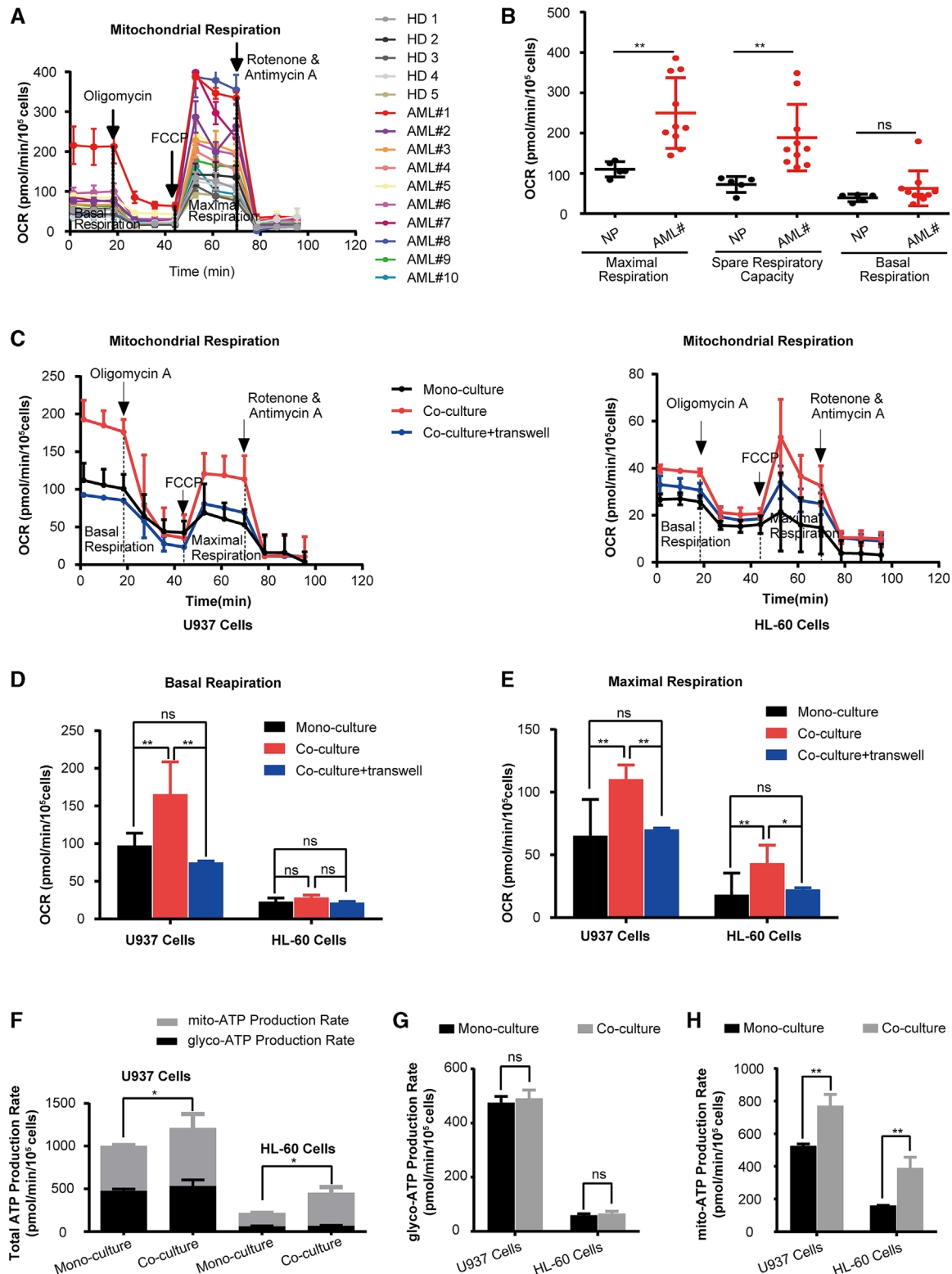


**FIGURE 1** Coculture of AML cells with HS-5 cells exhibited higher OXPHOS activity and increased ATP synthesis. (A) Sequential injections of oligomycin, FCCP, and rotenone/antimycin were used to obtain mitochondrial respiration dynamics of CD34<sup>+</sup> cells from the BM of AML patients and healthy donors ( $n = 10$  for AML patients;  $n = 5$  for healthy donors). (B) The mitochondrial basal respiration, maximal respiration, and spare respiratory capacity of CD34<sup>+</sup> cells from the BM of AML patients and healthy donors were analyzed with cell numbers normalized. (C) Sequential administration of oligomycin, FCCP, and rotenone/antimycin were used to obtain mitochondrial respiration dynamics of AML cells. (D-E) AML cells were cultured with HS-5 cells in a contact or non-contact co-culture system and then the mitochondrial basal and maximal respiration of AML cells were analyzed with cell numbers normalized. (F-H) AML cells were cultured with or without HS-5 cells and then the ATP production Capacity was analyzed with cell numbers normalized. (F) Total ATP production rate, (G) glycolytic, and (H) mitochondrial ATP production rates in AML cells. The data represent the mean  $\pm$  SD of 3 independent experiments with 3 replicates for each experiment. AML#, AML patients; HD, healthy donors. ns, no significant difference, \* $P < 0.05$ , \*\* $P < 0.01$ , \*\*\* $P < 0.001$

ing in “co-U937” and “co-HL-60 cells”, respectively). Interestingly, co-U937 cells exhibited increased basal and maximal respiration, and co-HL-60 cells showed increased maximal respiration, compared to the cells without co-culturing with HS-5 cells (mono-U937 or mono-HL-60 cells). Besides, we found that the direct co-cultured AML cells had significantly higher OXPHOS activity than non-contact co-cultured AML cells (Fig. 1C-E). Therefore, we chose the direct contact co-culture system for all the subsequent experiments.

Since the main function of mitochondrial OXPHOS is to produce ATP for cell growth, a real-time ATP production rate assay was carried out. As expected, co-AML cells had increased total ATP production compared to mono-AML cells (Fig. 1F). ATP in the cell is synthesized by two mechanisms, that is, mitochondrial respiration and glycolysis. To explore whether the increase of ATP production in co-AML cells was due to a higher level of mitochondrial OXPHOS, the mitochondrial ATP and glycolytic ATP production were separately evaluated. While glycolytic ATP production did not significantly differ between mono- and co-AML cells (Fig. 1G), the mitochondrial ATP production was significantly increased in co-AML cells compared to mono-AML cells (Fig. 1H). This suggested that AML cells co-cultured with HS-5 cells depended on mitochondrial OXPHOS for increasing ATP synthesis.

### 3.2 | Coculture of AML cells with HS-5 cells displayed decreased sensitivity to chemotherapy due to increased ATP synthesis

Co-AML cells showed decreased sensitivity to chemotherapy, as evidenced by the decreased drug-induced growth inhibitory and apoptosis (Fig. 2A and B). To investigate the role of mitochondrial ATP synthesis in the acquisition of chemotherapy resistance, Oligomycin A, a mitochondrial ATPase inhibitor, was employed to inhibit mitochondrial OXPHOS-mediated ATP synthesis. After treatment of AML cells with 10  $\mu$ M Oligomycin A that did not impair the viability of AML cells (Supplementary Fig. 2A-C), the mitochondrial ATP synthesis was significantly reduced (Fig. 2C). The sensitivity to chemotherapy was then tested under these conditions. Notably, Oligomycin A significantly increased the chemosensitivity of co-AML cells, but it did not significantly affect that of mono-AML cells (Fig. 2D and E). We further explored the impact of Oligomycin A on the total ATP level of AML cells. As shown in Fig. 2F, Oligomycin A significantly decreased the total ATP production in co-AML cells, while it had no effect on that of mono-AML cells. Moreover, we found that the inhibition of mitochondrial ATP synthesis led to a compensatory increase of glycolytic ATP synthesis in mono-AML cells (Fig. 2G), but similar effect was not observed in co-U937 cells (Fig. 2F). Although the glycolytic ATP production increased in co-HL-60 cells, it was not enough to compensate for the lack of mitochondrial ATP production after Oligomycin A treatment. Our data indicated that the increased ATP synthesis was associated with the reduced AML cells chemosensitivity, and the increase of ATP synthesis was strongly dependent on mitochondrial OXPHOS in the AML cells co-cultured with HS-5 cells.

### 3.3 | AMPK activity was inhibited by increased ATP synthesis in AML cells co-cultured with HS-5 cells

We next investigate the molecular link between increased ATP synthesis and the reduced sensitivity of co-AML cells to chemotherapy. AMPK activity is influenced by the AMP/ATP ratio, and mTORC1 activity is repressed by the AMPK checkpoint. Because p70S6K and 4E-BP1 are the direct substrates of mTORC1, mTORC1 activity was evaluated by analyzing the expression levels of p-p70S6K<sup>T389</sup> and p-4E-BP1<sup>S65</sup>. In the co-AML cells, the expression of p-AMPK<sup>T172</sup> (AMPK phosphorylation) was reduced, while p-p70S6K<sup>T389</sup> and p-4E-BP1<sup>S65</sup> were increased (Fig. 3A). Moreover, we observed increased expression of c-Myc, which are well-known downstream of mTORC1 (Fig. 3A). These results suggested that AMPK activity was inhibited, while mTORC1 signaling was up-regulated in co-AML cells.

We next investigated whether the reduced AMPK activity was caused by the elevated ATP production. When we treated co-AML cells with Oligomycin A to inhibit mitochondrial ATP synthesis, AMPK activity was increased, while mTORC1 was inhibited (Fig. 3B). Intriguingly, Oligomycin A treatment did not affect AMPK or mTORC1 activity in mono-AML cells (Fig. 3B). These findings suggested that the elevated mitochondrial ATP synthesis was a causative reason for AMPK inhibition, and in turn mTORC1 activation in co-AML cells.

### 3.4 | AMPK inhibition mediated AML cells chemoresistance induced by HS-5 cells

Since AMPK functions as a metabolic sensor for ATP status in the cells, we further investigate the role of AMPK inhibition in stromal cells-induced chemoresistance. The impact of AMPK modulation with chemical reagents on AML cells in response to chemotherapy was assessed. Treatment with AICAR, an AMPK agonist, could partially restore the sensitivity of AML cells to chemotherapy in the co-culture system (Fig. 4A and B). It may be noteworthy that while treatment of mono-U937 cells with 1 mM AICAR increased the growth inhibition rate of 200 ng/mL DNR only by approximately 4% ( $P < 0.05$ ), it may still support the notion that activation of AMPK can sensitize AML cells to the commonly used anti-leukemic drugs. On the contrary, treatment with Compound C, an AMPK antagonist, significantly reduced the sensitivity of AML cells to chemotherapy (Fig. 4C and D). These results suggested that AMPK inhibition played a key role in the chemoresistance of co-AML cells.

To further explore the role of AMPK in AML cells' response to chemotherapy, AMPK expression was suppressed in U937 cells by employing an AMPK-CRISPR/Cas9 construct. AMPK knockout induced a significant decrease in the sensitivity of mono- and co-AML cells to chemotherapy (Fig. 4E and F). However, AMPK overexpression in U937 cells did not significantly affect their chemosensitivity (Fig. 4G and H), probably because AMPK overexpression failed to increase AMPK activity, and did not affect the mTORC1 activity (Fig. 5A).

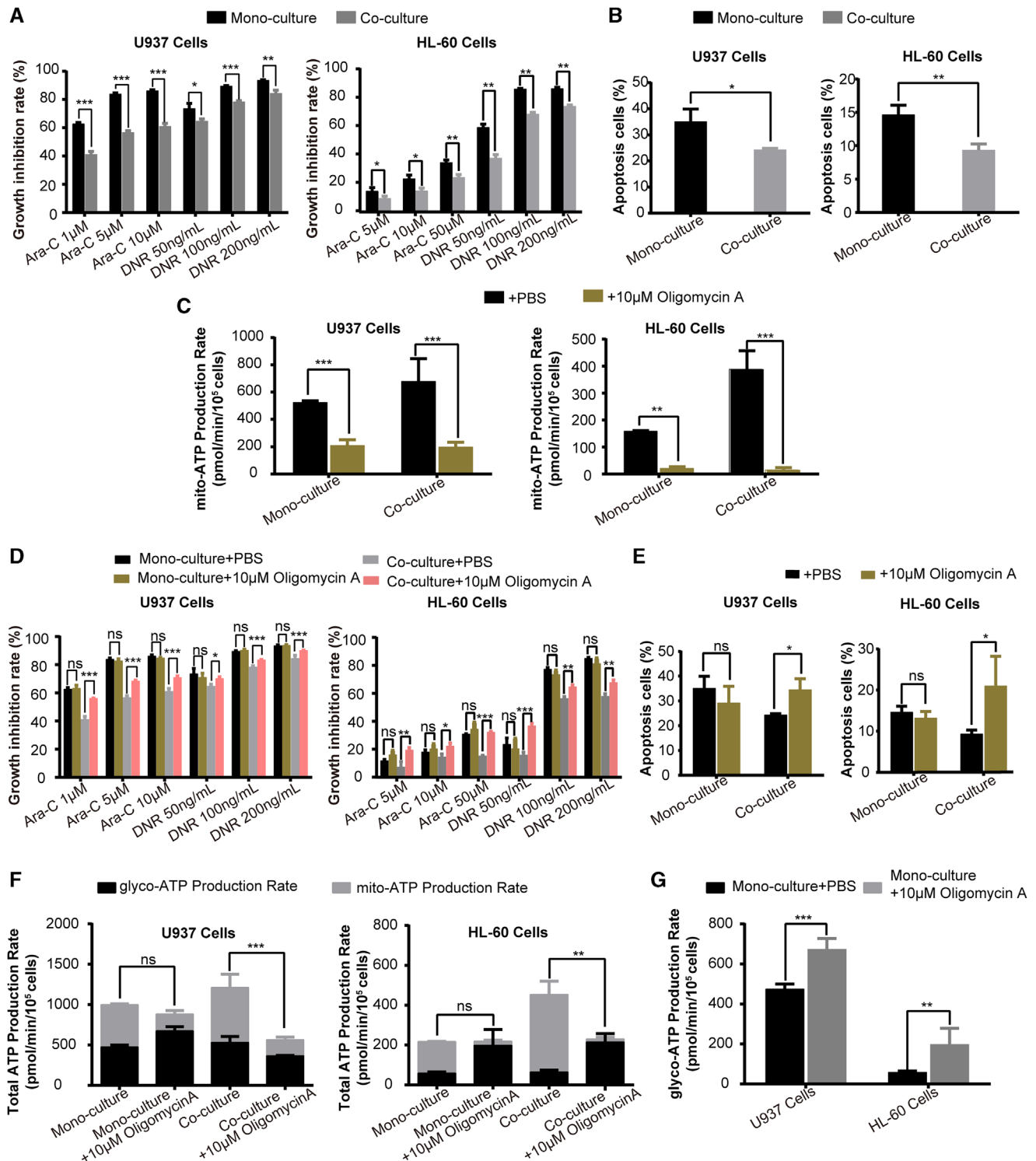


**FIGURE 2** Coculture of AML cells with HS-5 cells displayed the decreased sensitivity to chemotherapy due to the increased ATP synthesis. (A) Growth inhibitory effect of 24 h treatment with different concentrations of Ara-C and DNR on AML cells cultured alone or with HS-5 cells was measured by CCK-8 assay. (B) The percentage of apoptotic cells of 24 h treatment with Ara-C (The concentration of Ara-C was 50 µM for HL-60 cells and 5 µM for U937 cells) on AML cells cultured alone or with HS-5 cells was expressed as mean ± SD from 3 independent experiments. (C) The mitochondrial ATP production rate of AML cells was significantly inhibited by treatment with Oligomycin A. (D) Growth inhibitory effect of 24 h treatment with different concentrations of Ara-C and DNR on AML cells after treatment with 10 µM Oligomycin A was measured by CCK-8 assay. (E) The percentage of apoptotic cells of 24 h treatment with Ara-C (The concentration of Ara-C was 50 µM for HL-60 cells and 5 µM for U937 cells) on AML cells after treatment with 10 µM Oligomycin A was expressed as mean ± SD from 3 independent experiments. (F) Total ATP production rate and (G) glycolytic ATP production rate in AML cells after treatment with Oligomycin A. The data represent the mean ± SD of 3 independent experiments with 3 replicates for each experiment. AML#, AML patients. ns, no significant difference, \* $P < 0.05$ , \*\* $P < 0.01$ , \*\*\* $P < 0.001$

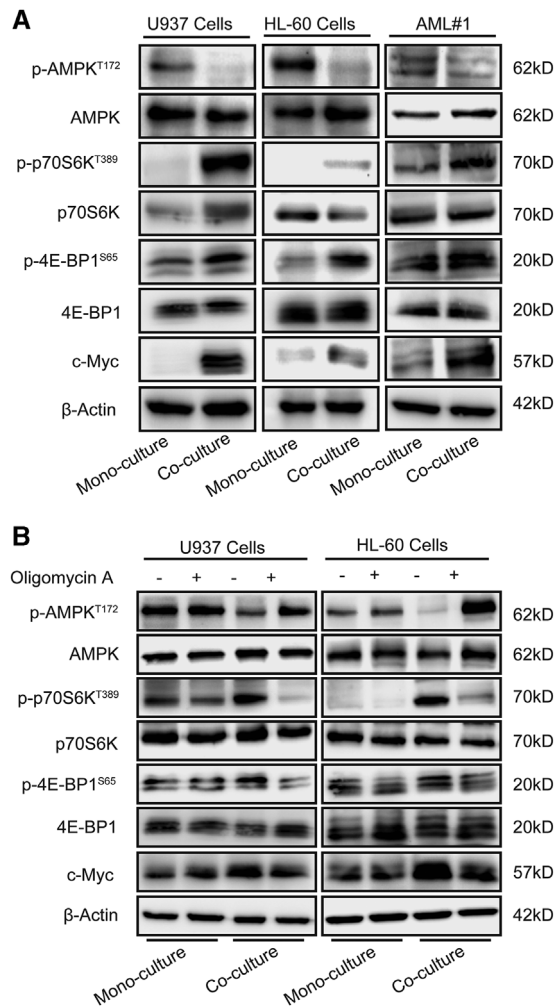


**FIGURE 3** AMPK activity was inhibited by increased ATP synthesis in AML cells co-cultured with HS-5 cells. (A) Representative western blot analysis of proteins involved in the AMPK-mTORC1 pathway (total AMPK, p-AMPK<sup>T172</sup>, total p70S6K, p-p70S6K<sup>T389</sup>, total 4E-BP1, p-4E-BP1<sup>S65</sup>, and c-Myc; β-actin was used as loading control) from AML cells cultured alone or with HS-5 cells. The expression levels of p-p70S6K<sup>T389</sup> and p-4E-BP1<sup>S65</sup> were used as indicators of mTORC1 activity. (B) Representative western blot analysis of AMPK-mTORC1 pathway proteins of AML cells after treatment with 10 μM Oligomycin A. The representative images of 3 independent experiments were used

### 3.5 | AMPK inhibition increases mTORC1 activity and c-Myc proteins expression

In co-AML cells, AMPK knockout resulted in the up-regulation of p-p70S6K<sup>T389</sup>, p-4E-BP1<sup>S65</sup>, and c-Myc proteins (Fig. 5B). Moreover, in co-AML cells, AICAR reduced the expression of p-p70S6K<sup>T389</sup> and p-4E-BP1<sup>S65</sup> and c-Myc (Fig. 5C), while Compound C increased the expression levels of p-p70S6K<sup>T389</sup>, p-4E-BP1<sup>S65</sup>, and c-Myc (Fig. 5D), suggesting that the chemoresistance effect of AMPK inhibition is probably mediated via activating mTORC1. Of note, c-Myc expression was dramatically increased in co-U937 cells treated with Compound C whereas moderate up-regulation of c-Myc was observed in co-HL-60 cells. This discrepancy might be due to cell-type speci-

ficity. In general, AMPK inhibition and the subsequent augmentation of mTORC1 activity, blocked the chemotherapy sensitivity in co-AML cells.

### 3.6 | AMPK knockout promoted AML progression and chemoresistance in mice

Although the role of the AMPK inhibition in the chemoresistance of AML cells was demonstrated in the in vitro assays, the impact of AMPK activity on in vivo AML progression and chemosensitivity remained to be determined. To address this issue, a xenograft model of AML was developed in NCG mice by using U937 leukemic cells with knockout of AMPK expression. The femurs, spleens, and livers of AML mice were analyzed.

The vascular structures were dramatically damaged in the femoral BM of U937<sup>AMPK-sg1</sup> mice, differently from those of U937<sup>WT</sup> and U937<sup>NC-sg</sup> mice (Fig. 6A), indicating a severe disease invasion. A higher leukemia burden in femoral BM was observed in U937<sup>AMPK-sg1</sup> mice (Fig. 6A-D), than that in the U937<sup>WT</sup> and U937<sup>NC-sg</sup> mice. Moreover, a higher rate of AML engraftment in the extramedullary organs and a more prominent splenomegaly were observed in U937<sup>AMPK-sg1</sup> mice compared with other groups (Fig. 6E-H; Supplementary Fig. 1). These results collectively suggested that AMPK inhibition promotes AML progression in vivo.

Finally, we assessed the impact of AMPK inhibition on sensitivity of AML mice to Ara-C. Consistent with the results from in vitro chemosensitivity testing, AMPK inhibition in the mouse model also significantly reduced chemosensitivity in vivo (Figs 6I and J), suggesting that AMPK inhibition is essential not only to promote AML progression, but also to facilitate chemoresistance.

## 4 | DISCUSSION

AML cells are characterized by their intimate contact with the stromal microenvironment in the BM.<sup>27,28</sup> This interaction protects malignant cells from spontaneous apoptosis, promotes proliferation and drug resistance.<sup>9,29</sup> But the precise molecular details of this interaction remain elusive. Here, we found that co-culturing with HS-5 cells, a type of BMM-derived stromal cells, rendered AML cells resistant to chemotherapy via elevating OXPHOS activity and mitochondrial ATP synthesis of AML cells. To explore that the increase of OXPHOS-mediated ATP production induced by HS-5 cells is an important factor affecting the chemoresistance of AML cells, Oligomycin A, the mitochondrial ATP synthase inhibitor, was employed to inhibit the mitochondrial ATP production of AML cells. We found that treatment of co-AML cells with Oligomycin A enhanced their sensitivity to Ara-C and DNR while having no effect on mono-AML cells, and that such potentiating effect resulted from the decreased total ATP production in co-AML cells. These results clearly suggest that BMM-induced reprogramming of energy metabolism in AML cells was involved in the acquisition of chemotherapy resistance. Although the involvement of energy

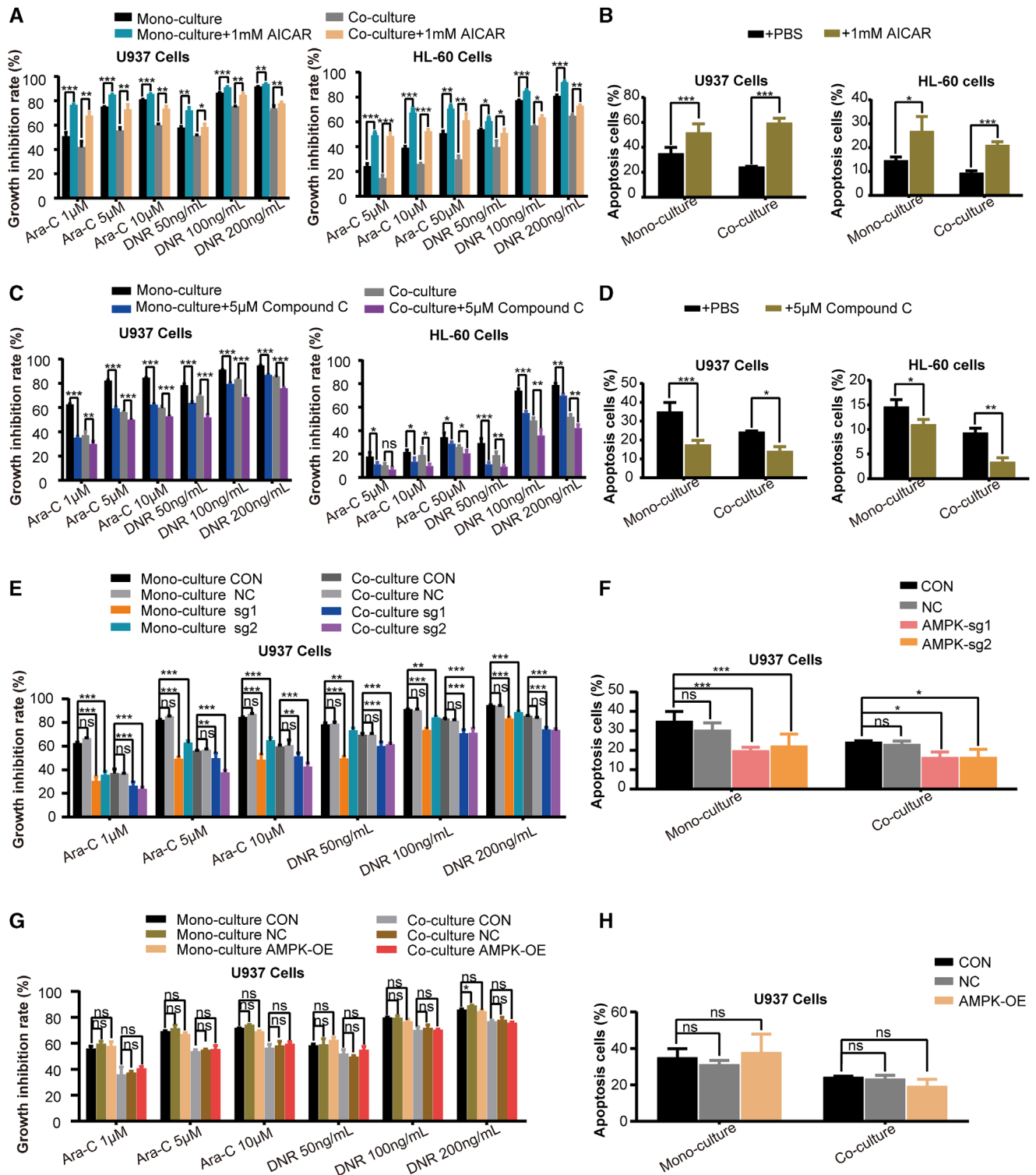


**FIGURE 4** AMPK inhibition mediated the chemoresistance of AML cells induced by HS-5 cells. (A) Growth inhibitory effect of 24 h treatment with different concentrations of Ara-C and DNR on AML cells after treatment with 1 mM 5-aminoimidazole-4-carboxamide ribonucleotide (AICAR) was measured by CCK-8 assay. (B) The percentage of apoptotic cells of 24 h treatment with Ara-C (The concentration of Ara-C was 50 μM for HL-60 cells and 5 μM for U937 cells) on AML cells after treatment with 1 mM AICAR was expressed as mean ± SD from 3 independent experiments. (C) Growth inhibitory effect of 24 h treatment with different concentrations of Ara-C and DNR on AML cells after treatment with 5 μM Compound C was measured by CCK-8 assay. (D) The percentage of apoptotic cells of 24 h treatment with Ara-C (The concentration of Ara-C was 50 μM for HL-60 cells and 5 μM for U937 cells) on AML cells after treatment with 5 μM Compound C was expressed as mean ± SD from 3 independent experiments. (E) Growth inhibitory effect of 24 h treatment with different concentrations of Ara-C and DNR on U937 cells knocked out for AMPK was measured by CCK-8 assay. (F) The percentage of apoptotic cells of 24 h treatment with Ara-C (The

(Continues)

**FIGURE 4** (Continued)

concentration of Ara-C was  $50\mu\text{M}$  for HL-60 cells and  $5\mu\text{M}$  for U937 cells) on U937 cells knocked out for AMPK was expressed as mean  $\pm$  SD from 3 independent experiments. (G) Growth inhibitory effect of 24 h treatment with different concentrations of Ara-C and DNR on AMPK-overexpressing U937 cells. (H) The percentage of apoptotic cells of 24 h treatment with Ara-C on AMPK-overexpressing U937 cells was expressed as mean  $\pm$  SD from 3 independent experiments. The data represent the mean  $\pm$  SD of 3 independent experiments with 3 replicates for each experiment. CON, wide type; NC, empty vector control; AMPK-OE, AMPK overexpression; AMPK-sg1/2, AMPK gene was knocked out. ns, no significant difference, \* $P < 0.05$ , \*\* $P < 0.01$ , \*\*\* $P < 0.001$

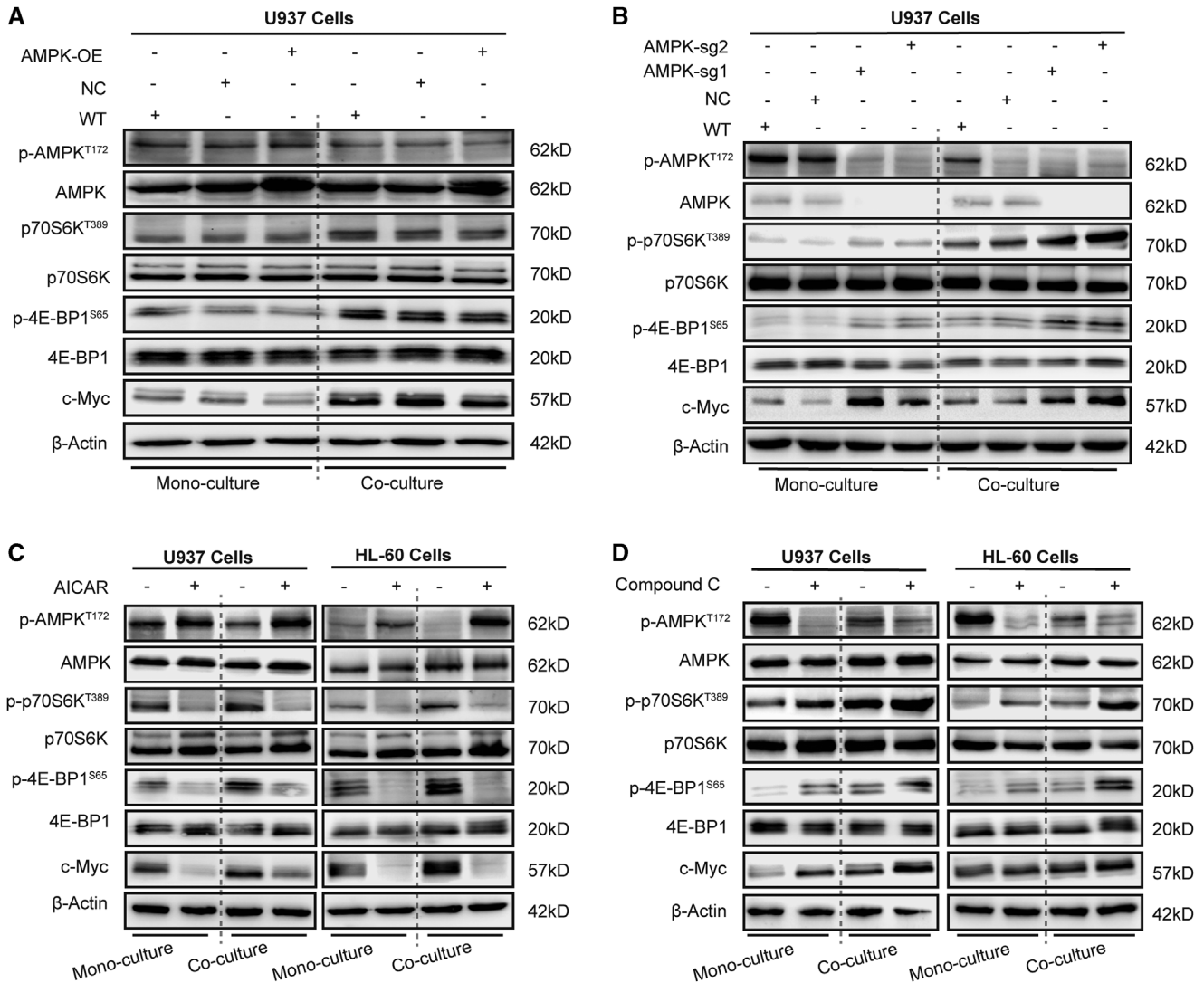


**FIGURE 5** AMPK inhibition increases mTORC1 activity and c-Myc proteins expression. (A) Representative western blot analysis of AMPK-mTORC1 pathway proteins (total AMPK, p-AMPK<sup>T172</sup>, total p70S6K, p-p70S6K<sup>T389</sup>, total 4E-BP1, p-4E-BP1<sup>S65</sup>, and c-Myc;  $\beta$ -actin was used as loading control) of AMPK-overexpressing U937 cells. (B) Representative western blot analysis of AMPK-mTORC1 pathway proteins in U937 cells knocked out for AMPK expression. (C) Representative western blot analysis of AMPK-mTORC1 pathway proteins from AML cells after treatment with 1 mM AICAR. (D) Representative western blot analysis of AMPK-mTORC1 pathway proteins in AML cells after treatment with 5  $\mu\text{M}$  Compound C. WT, wide type; NC, empty vector control; AMPK-OE, AMPK overexpression; AMPK-sg1/2, AMPK gene was knocked out. The representative images of 3 independent experiments were used

metabolism in leukemia chemoresistance has been proposed by previous studies,<sup>16,30</sup> how energy surplus in AML cells regulates chemoresistance of AML cells has not been studied.

Our study provides novel insights into the molecular pathways linking energy metabolism reprogrammed by BMM in AML cells to

chemoresistance. AMPK is not only a central regulator of energy homeostasis but also is an important energy sensor that is affected by the AMP/ATP ratio in cell. We further showed evidence supporting that the increased OXPHOS and mitochondrial ATP synthesis in AML cells caused the inhibition of AMPK, which in turn promotes mTORC1

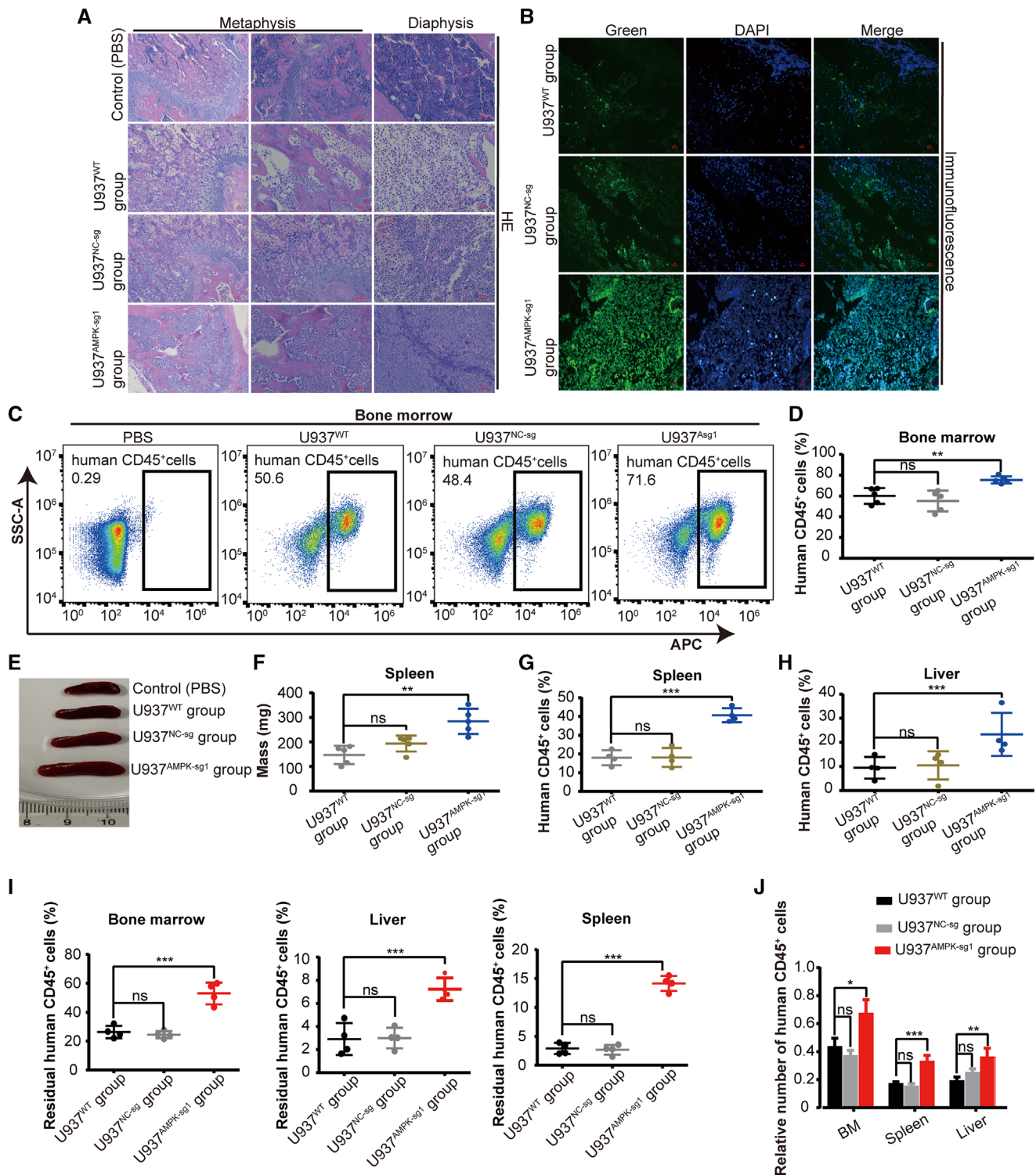


**FIGURE 6** AMPK knockout cells promoted AML progression and chemoresistance in mice. (A) Hematoxylin and eosin (HE) staining of the femurs from NCG mice. Scale bar, 50  $\mu$ M. (B) Immunofluorescence (IF) staining for human CD45 (green) expression and nuclei marker (DAPI, blue) in the femurs of NCG mice. Scale bar, 50  $\mu$ M. (C) Representative FCM profiles of human CD45 surface marker expression in AML cells of femurs. (D) Each data point represents the proportion of human CD45<sup>+</sup> cells in the femurs per mouse (n = 5). (E-F) Spleen anatomy (E) and weight (F) in the control, U937<sup>WT</sup>, U937<sup>NC-sg</sup>, and U937<sup>AMPK-sg1</sup> mice (n = 5). (G-H) Each data point represents the proportion of human CD45<sup>+</sup> cells in the spleens (G) and livers (H) per mouse (n = 4). (I) Each data point represents the proportion of residual human CD45<sup>+</sup> cells in the femur, spleen, and liver per mouse after Ara-C treatment (n = 4). (J) The relative number of human CD45<sup>+</sup> cells after Ara-C treatment was normalized to vehicle-treated controls. WT, wide type; NC-sg, empty vector control; AMPK-sg1, AMPK gene was knocked out. ns, no significant difference, \*P < 0.05, \*\*P < 0.01, \*\*\*P < 0.001

activation and the translation of proteins involved in cell growth and survival. Collectively, BMM induced AML cells to rely on mitochondrial OXPHOS to produce ATP for energy supply, which inhibited AMPK activity and in return upregulated mTORC1 activity, eventually promoting AML cell chemoresistance. This implied that AMPK-mTORC1 pathway integrated information about the availability of energy to coordinate the synthesis or breakdown of cellular components (e.g., some proteins).

The structure and function of AMPK protein have aroused great interest since it is understood that AMPK protein acts as the central regulator of intracellular energy homeostasis. It is noteworthy that the role of AMPK in the progression of cancers including leukemia is controversial. A study reports that AMPK inhibits tumor growth in oxidative stress<sup>31</sup> whereas other studies demonstrate that AMPK promotes tumor growth.<sup>32,33</sup> Although the exact role of AMPK in AML remains elusive, this study identifies a novel mechanism by which AML cells develop resistance to anti-leukemic drugs. The lack of AMPK activity due to knocking out AMPK in AML cells activated mTORC1 signaling and reduced the chemosensitivity of AML cells. Similar to the *in vitro*, a xenograft model of human AML cells was carried out in NCG mice and we found that lack of AMPK activity promoted AML progression and reduced their sensitivity to chemotherapeutic drugs, indicating that AMPK had a tumor suppressor effect in AML. Unexpectedly, we found that overexpression of AMPK did not alter the chemosensitivity of AML cells. A plausible explanation might lie in the fact that AMPK acts mainly through its activity,<sup>34</sup> which coincides with the increase/decrease in chemosensitivity of AML cells after treatment with AICAR/Compound C. To further confirm this, we explored the changes of AMPK-mTORC1 signaling pathway after AMPK overexpression in AML cells, and found that AMPK overexpression did not lead to an increase in AMPK activity, confirming that it is the activity of AMPK rather than its protein levels that accounts for the chemosensitivity of AML cells.

In addition, AMPK has been reported by previous studies to be associated with survival and proliferation of AML cells,<sup>20,35</sup> but most of these studies did not directly link AMPK with the chemosensitivity of AML. To date, only one previous report has linked AMPK to drug sensitivity in AML. That study found that activation of the AMPK-ULK1 signaling pathway reduces the sensitivity of AML to bromodomain and extraterminal domain (BET) inhibitors, independent of the mTOR pathway.<sup>36</sup> In our present study, gain-in-function and loss-of function experiments that did not result in AML cells apoptosis have verified that, when co-cultured with BMSCs, AMPK inhibition promoted mTORC1 hyper-activation to mediate chemoresistance. The mTORC1 hyper-activation was associated with the increase of c-Myc, which were supposed to contribute to the chemoresistance. Our work thus highlighted the importance of AMPK-mTORC1 axis in AML chemoresistance and suggested a promising therapeutic opportunity through intervening AMPK and mTORC1 activity in AML.

It is interesting to determine how BMM reprograms energy metabolism in AML cells. Previous studies have also reported that BMM could increase mitochondria mass and promote OXPHOS activity of AML cells, eventually leading to chemoresistance.<sup>15,37</sup> Our

results showed that OXPHOS activity was increased after contact coculture, but not after transwell-coculture, indicating that direct contact with stromal cells was essential to increase OXPHOS activity in AML cells. The exact mechanism of BMM-mediated AML cell energy metabolism reprogramming warrants further investigation.

In conclusion, our work reveals the role of OXPHOS/AMPK/mTORC1 pathway on linking energy metabolism reprogramming to AML chemoresistance induced by BMM. Blocking the crosstalk between BMM and AML cells, or interfering with energy metabolism in AML, may represent novel therapeutic strategies to treat the chemoresistant leukemia.

## ACKNOWLEDGMENT

This work was supported by the National Natural Science Foundation of China (81870108, 82070145, 81800136), the Fujian Medicine Innovation Program (2018-CX-18), Joint Funds for the innovation of science and Technology, Fujian province (2017Y9053, 2019Y9073), Fujian Province Natural Science Foundation (2020J01991), the government-funded project of the construction of high-level laboratory and the construction project of Fujian medical center of hematology (Min201704) and National and Fujian Provincial Key Clinical Specialty Discipline Construction Program, P. R.C.

## DISCLOSURE

The authors declare no conflict of interest.

## AUTHORSHIP

H.-F.H. secured funding, conceived the project, designed the experiments. R.-L.Y. performed the majority of experiments and wrote the manuscript. D.-Y.H and B.W helped to search the literature. J.-R.L., X.-T.W., Q.-R.X., and Z.-P.P. helped to create the figures and tables. D.-L.L., X.-M.F., L.-X.K., and P.C. provided critical inputs, and guidance for experiments.

## ETHICS APPROVAL AND CONSENT TO PARTICIPATE

A statement that the study was performed in accordance with the Declaration of Helsinki. This study involving human specimens was approved by the Committee for the Ethical Review of Research, Fujian Medical University Union Hospital (2018KY061). All experiments involving animals were performed according to protocols approved by the Committee of Research Animals of Fuzhou General Hospital of Nanjing Military Command (2020-044).

## REFERENCES

1. Ferrara F, Schiffer CA. Acute myeloid leukaemia in adults. *Lancet*. 2013;381:484-95.
2. Short NJ, Rytting ME, Cortes JE. Acute myeloid leukaemia. *Lancet*. 2018;392:593-606.
3. O'Dwyer K, Freyer DR, Horan JT. Treatment strategies for adolescent and young adult patients with acute myeloid leukemia. *Blood*. 2018;4:362-8.
4. Dohner H, Estey EH, Amadori S, Appelbaum FR, Buchner T, Burnett AK, et al. Diagnosis and management of acute myeloid leukemia in adults: recommendations from an international expert panel, on behalf of the European LeukemiaNet. *Blood*. 2010;115:453-74.

5. Shlush LI, Mitchell A, Heisler L, Abelson S, Ng SWK, Trotman-Grant A, et al. Tracing the origins of relapse in acute myeloid leukaemia to stem cells. *Nature*. 2017;547:104-8.
6. Thomas D, Majeti R. Biology and relevance of human acute myeloid leukemia stem cells. *Blood*. 2017;129:1577-85.
7. Crane GM, Jeffery E, Morrison SJ. Adult haematopoietic stem cell niches. *Nat Rev Immunol*. 2017;17:573-90.
8. Shafat MS, Gnanaswaran B, Bowles KM, Rushworth SA. The bone marrow microenvironment - Home of the leukemic blasts. *Blood Rev*. 2017;31:277-86.
9. Duarte D, Hawkins ED, Lo Celso C. The interplay of leukemia cells and the bone marrow microenvironment. *Blood*. 2018;131:1507-11.
10. Tamplin OJ. Chewing through Roots: how Leukemia Invades and Disrupts the Bone Marrow Microenvironment. *Cell Stem Cell*. 2018;22:5-7.
11. Hanahan D, Weinberg RA. Hallmarks of cancer: the next generation. *Cell*. 2011;144:646-74.
12. DeBerardinis RJ, Chandel NS. Fundamentals of cancer metabolism. *Science Advances*. 2016;5:e1600200.
13. Icard P, Shulman S, Farhat D, Steyaert JM, Alifano M, Lincet H. How the Warburg effect sorts aggressiveness and drug resistance of cancer cells?. *Drug Resist Updat*. 2018;38:1-11.
14. Counihan JL, Grossman EA, Nomura DK. Cancer metabolism: current understanding and therapies. *Chem Rev*. 2018;118:6893-923.
15. Farge T, Saland E, de Toni F, et al. Chemotherapy-resistant human acute myeloid leukemia cells are not enriched for leukemic stem cells but require oxidative metabolism. *Cancer Discovery*. 2017;7:716-35.
16. Henkenius K, Greene BH, Barckhausen C, et al. Maintenance of cellular respiration indicates drug resistance in acute myeloid leukemia. *Leukemia Research*. 2017;62:56-63.
17. Garcia D, Shaw RJ. AMPK: mechanisms of cellular energy sensing and restoration of metabolic balance. *Mol Cell*. 2017;66:789-800.
18. Gonzalez A, Hall MN, Lin SC, Hardie DG. AMPK and TOR: the Yin and Yang of cellular nutrient sensing and growth control. *Cell Metab*. 2020;31:472-92.
19. Jiang Y, Nakada D. Cell intrinsic and extrinsic regulation of leukemia cell metabolism. *Int J Hematol*. 2016;103:607-16.
20. Green AS, Chapuis N, Maciel TT, et al. The LKB1/AMPK signaling pathway has tumor suppressor activity in acute myeloid leukemia through the repression of mTOR-dependent oncogenic mRNA translation. *Blood*. 2010;116:4262-73.
21. Kim J, Guan KL. mTOR as a central hub of nutrient signalling and cell growth. *Nat Cell Biol*. 2019;21:63-71.
22. Liu GY, Sabatini DM. mTOR at the nexus of nutrition, growth, ageing and disease. *Nat Rev Mol Cell Biol*. 2020;21:183-203.
23. Dasgupta B, Chhipa RR. Evolving Lessons on the Complex Role of AMPK in Normal Physiology and Cancer. *Trends Pharmacol Sci*. 2016;37:192-206.
24. Shin JM, Jeong YJ, Cho HJ, Magae J, Bae YS, Chang YC. Suppression of c-Myc induces apoptosis via an AMPK/mTOR-dependent pathway by 4-O-methyl-ascoclhorin in leukemia cells. *Apoptosis*. 2016;21:657-68.
25. Hoshii T, Tadokoro Y, Naka K, et al. mTORC1 is essential for leukemia propagation but not stem cell self-renewal. *J Clin Invest*. 2012;122:2114-29.
26. Liang JR, Lingeman E, Luong T, et al. A Genome-wide ER-phagy screen highlights key roles of mitochondrial metabolism and ER-resident UFMylation. *Cell*. 2020;180:e20.
27. Ayala F, Dewar R, Kieran M, Kalluri R. Contribution of bone microenvironment to leukemogenesis and leukemia progression. *Leukemia*. 2009;23:2233-41.
28. Braun M, Qorraj M, Buttner M, et al. CXCL12 promotes glycolytic reprogramming in acute myeloid leukemia cells via the CXCR4/mTOR axis. *Leukemia*. 2016;30:1788-92.
29. Schepers K, Campbell TB, Passegue E. Normal and leukemic stem cell niches: insights and therapeutic opportunities. *Cell Stem Cell*. 2015;16:254-67.
30. Baccelli I, Gareau Y, Lehnertz B, et al. Mubritinib targets the electron transport chain complex I and reveals the landscape of OXPHOS dependency in acute myeloid leukemia. *Cancer Cell*. 2019;36:84-99. e8.
31. Faubert B, Boily G, Izreig S, et al. AMPK is a negative regulator of the Warburg effect and suppresses tumor growth in vivo. *Cell Metab*. 2013;17:113-24.
32. Jeon SM, Chandel NS, Hay N. AMPK regulates NADPH homeostasis to promote tumour cell survival during energy stress. *Nature*. 2012;485:661-5.
33. Saito Y, Chapple RH, Lin A, Kitano A, Nakada D. AMPK protects leukemia-initiating cells in myeloid leukemias from metabolic stress in the bone marrow. *Cell Stem Cell*. 2015;17:585-96.
34. Carling D. AMPK signalling in health and disease. *Curr Opin Cell Biol*. 2017;45:31-7.
35. Pei S, Minhajuddin M, Adane B, et al. AMPK/FIS1-mediated mitophagy is required for self-renewal of human AML stem cells. *Cell Stem Cell*. 2018;23:86-100. e6.
36. Jang JE, Eom JI, Jeung HK, et al. Targeting AMPK-ULK1-mediated autophagy for combating BET inhibitor resistance in acute myeloid leukemia stem cells. *Autophagy*. 2017;13:761-2.
37. Moschoi R, Imbert V, Nebout M, et al. Protective mitochondrial transfer from bone marrow stromal cells to acute myeloid leukemic cells during chemotherapy. *Blood*. 2016;128:253-64.

## SUPPORTING INFORMATION

Additional supporting information may be found in the online version of the article at the publisher's website.

**How to cite this article:** You R, Hou D, Wang B, et al. Bone marrow microenvironment drives AML cell OXPHOS addiction and AMPK inhibition to resist chemotherapy. *J Leukoc Biol*. 2022;112:299-311.

<https://doi.org/10.1002/JLB.6A0821-409RR>